The structural effects on silver nanoparticles plasma edges in optical reflectance spectra of Ag/Ag_2O composites synthesized by oxygen plasma treatment of silver thin films

Kamal Hamed Kayed (khmk2000@gmail.com)
Damascus University https://orcid.org/0000-0001-9842-9080

Research Article

Keywords: Silver Oxide, Plasma edge, Individual silver nanoparticles, Thermal evaporation, Oxygen plasma afterglow, Reflection spectra, Inhibition of bacteria

Posted Date: October 7th, 2021

DOI: https://doi.org/10.21203/rs.3.rs-932156/v1

Abstract

In this work, we present the results of a unique study that aims to detect the structural effects on the plasma edges in optical reflectance spectra of Ag/Ag_2O composites synthesized by treating silver thin films manufactured by thermal evaporation method with oxygen plasma afterglow. The results showed that, each of the optical reflectance spectra contains two plasma edges, the first (λ_I) belongs to the surface plasmons of the individual silver nanoparticles, and the second (λ_L) belongs to the larger silver nanoparticles. In addition, we found that the positions of the plasma edges are linearly related to the positions of the optical absorption peaks, except for high and low oxidation rates cases. On the other hand, taking into account previous work, we obtained indications that, the ratio N_I/N_L may be a measure of the film's effectiveness in inhibiting bacteria.

1. Introduction

The increased interest of many research groups around the world in the synthesis and characterization of Ag/Ag_2O composites [1-13] is due to the unique modifications to the optical properties of silver oxide caused by the silver nanoparticles that are mainly related to the surface plasmon resonance (SPR) of silver nanoparticles [8]. The resonance effect occurs due to the interaction of the incident light with the electron density surrounding AgNPs [8].

In our previous work [14], we used oxygen plasma afterglow to treat silver thin films for the preparation of high quality Ag_2O thin films. The optical and structural properties of the prepared samples were investigated. The obtained results showed that, exposing silver thin films to oxygen plasma leads to a monocrystalline structure of cubic-Ag_2O phase. We found that, the silver oxide content increases with increasing of the plasma power in the region from 250 W to 1000 W. Otherwise, the treatment with plasma power of 1250 W leads to a decrease in the intensity of this peak. We also found that, the plasma power has significant effects on the characteristics of all plasmon resonance peaks (intensity, position and spectral width). On the other hand, a slight degradation of the individual silver nanoparticles plasmon peaks was recorded. It has been suggested that this decomposition occurs because of the mutual interaction between the individual silver nanoparticles located near Ag_2O grain shell and the larger Ag nanoparticles located in the neighboring grains. The results also showed that the degradation is degree related to the silver oxide grain size.

Optical reflectivity is considered one of the important physical property of the metal layers and metal/semiconductor composites, which relates to the interaction between the light photons and the free electrons which could be expressed by the equation [15,16]:

$$\omega_p = \sqrt{\frac{4\pi N e^2}{\varepsilon_\infty m^*}} \qquad (1)$$

Where ωp is the plasma edge, (N) is the conducting electrons concentration, (e) the electron charge, (ε_∞) dielectric constant and (m^*) the effective mass of the electron. The plasma edge is related to electrons concentration and electron effective mass [15], and could be determined from the optical reflecting spectra, where a dramatic increase in reflectivity happen at the wavelength of the plasma edge as a result of the photons reflection from the conduction band of the electron plasma oscillations [16]. Furthermore, equation 1 indicates that, when charge carrier concentration, the plasma edge shifts to high frequencies (shorter wavelengths) [16]. In this paper, we are interested in identifying the factors affecting the plasma edges formed in the optical reflectance spectra of Ag/Ag_2O composites synthesized by oxygen plasma treatment of silver thin films.

2. Experimental

2.1. Sample preparation

Pure silver metal thin films were deposited onto thoroughly cleaned n-type Si (100) and glass substrates from a high-purity Ag target by using thermal evaporation system (JSM200) at room temperature. The substrate placed above the target in the direction of the vapor flux. Table 1 contains the deposition parameters.

Table 1
The deposition parameters.

Deposition pressure	Deposition time	Target current	Deposition temperature	Target purity	The silver film thickness
$5x10^{-4}$ Pa	15 min	225 A	25●C	99.99%	316 nm

The oxidation process was done by placing each silver film in an evacuated Pyrex tube and exposing it to a stream of oxygen plasma afterglow at a specific plasma power. The oxygen plasma stream was generated by using Microwave SAIREM GMP 20 KEDS. More details about the plasma generation system are available in previous works [17–18]. Table 2 contains The conditions of oxygen plasma exposure for each sample.

Table 2
The conditions of oxygen plasma (afterglow) exposure for each sample.

Sample name	Plasma power	The film - discharge center distance	Plasma power	Oxygen plasmapressure	Processing time
A	250 W	0.25 m	250 W	300 Pa	30 min
B	500 W	0.25 m	500 W	300 Pa	30 min
C	750 W	0.25 m	750 W	300 Pa	30 min
D	1000 W	0.25 m	1000 W	300 Pa	30 min
E	1250 W	0.25 m	1250 W	300 Pa	30 min

2.2. Sample characterization

The crystallite structure of the prepared thin films was determined using (Stoe StadiP) transmission X-ray diffractometer employing a Cu $K\alpha_1$ source (λ = 1.54060 Å). The Raman spectra of silver oxide films were recorded using Micro Raman Jobin-Yvon (LabRAM HR) equipped with a laser source having an excitation wavelength of 514.5 nm. Scanning Electron Microscopy (TSCAN, Vega\\XMU) with SEM HV of 20 kV was performed to determine the thickness and the surface morphology of the prepared thin films. The optical absorption spectra was recorded by using a UV–Vis spectrophotometer (Cary 5000). The photoluminescence (PL) spectra were recorded at room temperature using a He–Cd laser with an excitation wavelength of 325 nm. A grating monochromator (1200 groves/mm) and cooled photomultiplier tube PMT, was also used to measure PL spectra. All PL spectra were fitted into two Gaussian–Lorentzian peaks to identify their position, spectral width and relative intensities.

3. Results And Discussion

The reflectance spectra of the oxygen plasma treated silver thin films are shown in Fig. 1.

We notice that, the reflectivity is at a maximum for the sample A that treated at 250 W, and when power of 500 W is applied (sample B), it decreases dramatically and then increases again as the plasma power increases. In this figure, it appears that the samples with low oxygen content have the highest values of reflectivity and that the spectra of the rest of the samples are within a narrow reflectivity range. These results demonstrate the diversity of mechanisms that control the optical reflection of the prepared samples. In the case of the samples A and E, high reflectivity is obtained due to the metallic nature of these samples that have a low content of oxygen [14]. As for the rest of the samples, the surface plasmon formation controls the overall optical properties, not just the optical reflectivity, and this is what we have seen in our previous works [14, 19–20]. The surface plasmons absorb or scatter the incident light. It seems that in the case of the sample B the absorption of light by the surface plasmons is dominant because the reflectivity near the edge of the plasma is low compared to the rest of the samples. As the plasma power increases (samples C and D), the reflectivity increases at the expense of the optical absorption.

In Fig. 1, it can be seen that there are two plasma edges in each spectrum, the first (λ_I) is located in the range 347-363 nm and belongs to the surface plasmons of the individual silver nanoparticles, and the second (λ_L) is located in the range 366-586 nm and it belongs to the larger silver nanoparticles. We previously obtained a similar case of plasma edge duality when studying the optical properties of aluminum oxide thin films prepared by thermal oxidation of aluminum films [21].Table 3 contains the values of plasma edges for all samples.

Table 3
The plasma edges values for all samples.

Sample label	λ_I (nm)	λ_L (nm)
A	347	366
B	352	413
C	362	468
D	363	586
E	348	364

The effect of the oxygen plasma power on the plasma edge is shown in Fig. 2. We notice that, for the two edges of the plasma, when the plasma power increases, the plasma edge increases exponentially until it reaches its maxima at p=1000W, and then decreases dramatically at p=1250W. This behavior is quite similar to that of the silver oxide content of the sample as a function of the plasma power, which we studied in previous work [14].We also notice that, the response of the λ_I edge to power changes is very small compared to the response of the λ_L edge.

Fig. 3 illustrates the plasma edge as a function of Ag_2O grain size. In this figure, one observes that the grain size increases with grain size. The effect of grain size on the (I) edge position is very small, while in the case of the (L) edge, the effect becomes obvious for sizes larger than 30 nm. Similar behavior is obtained when investigating the relationship between the edge position and silver oxide XRD peak intensity (the XRD spectra of the prepared samples were studied in detail in a previous work [14). These results can be explained based on the fact that, the increase in the film's oxygen content (which is associated with the increase in the size of the silver oxide grains [14]) leads to a decrease in the concentration of charge carriers and thus the shift of the plasma edge towards higher wavelengths (red-shift) as predicted by Equation 1.

In our previous work [14], we found that the optical absorption spectra of the prepared samples contain two main characteristic peaks: the peak (I), which belongs to the individual silver nanoparticles, and the peak (L), which belongs to the larger silver nanoparticles. It is important to investigate the relationship between the positions of these peaks and the positions of the plasma edges (I and L) inferred from optical reflectivity spectra. Fig. 5 represents the relationship between the positions of the absorption peaks and the positions of the plasma edges. An interesting result can be deduced from this figure, as we notice that the points of the two series are organized in a uniform linear relationship, except for two points in series L that represent the samples A and B. The point A of the L series does not belong to the straight line in Fig. 5 due to the dipole-dipole interactions that occur because this sample contains a high concentration of large Ag nanoparticles [14].On the other hand, sample D contains a relatively high oxygen content as a result of the oxidation of silver atoms. This results in polarized chemical bonds [20] and the polarization in turn affects the positions of both the absorption peaks and the plasma edges causing point D to move away from the straight line in Fig. 5.

Equation 1 describes both λ_I and λ_L plasma edges and can be used to calculate the ratio N_I/N_L. Where N_I is the charge carrier density for individual silver nanoparticles and N_L is the charge carrier density for larger silver nanoparticles. Fig. 6 shows the N_I/N_L ratio as a function of oxygen plasma power.

We notice that, the ratio N_I/N_L behaves similarly to the two edges of the plasma in Fig. 2, where when the plasma power increases, the ratio N_I/N_L increases exponentially until it reaches its maxima at p= 1000W, and then decreases dramatically at p= 1250W. This behavior is quite similar to that of the silver oxide content of the sample as a function of the plasma power, which we studied in previous work [14]. Based on this, we conclude that the ratio N_I/N_L increases with the increase in the concentration of Ag_2O oxide in the sample, (see the curve in Fig. 7, which shows the ratio N_I/N_L as functions of silver oxide XRD peak intensity). In other words, these results confirm that while the film content of large nanoparticles decreases due to oxide formation [14], the concentration of charge carriers in individual silver nanoparticles increases compared to the concentration of charge carriers in larger silver nanoparticles. We believe that the ratio N_I/N_L, which has a maximum value in sample D, is what gives this sample the highest activity to inhibit bacteria [22], and this supported by our previous findings that individual silver nanoparticles are a major factor in bacterial inhibition [22].

Finally, Figure 8 shows the ratio N_I/N_L as a function of particle size, as we notice that the ratio N_I/N_L increases with increasing particle size. The ratio N_I/N_L starts to increase significantly starting from a particle size of 30nm.

4. Conclusions

In this work, we are interested in investigating the structural effects on the plasma edges observed in the optical reflectivity spectra of Ag/Ag_2O composites synthesized by oxygen plasma treatment of silver thin films. We obtained unique results summarized in the following points:

1. Two types of plasma edges were observed in the reflectivity spectra of Ag/Ag_2O composites, the first (λ_I) belongs to the surface plasmons of the individual silver nanoparticles, and the second (λ_L) belongs to the larger silver nanoparticles.
2. Oxygen plasma power has a large effect on the silver nanoparticles edge plasma edge (λ_L) compared to its effect on the individual silver nanoparticles plasma edge (λ_I).
3. The increase in both the particle size and the film's oxygen content causes the plasma edges to shift towards higher wavelengths.
4. The positions of the plasma edges are linearly related to the positions of the optical absorption peaks, except for high and low oxidation rates cases.
5. Silver oxidation leads to a decrease in the concentration of charge carriers in the nanoparticles configurations, but at the same time leads to an increase in the ratio N_I/N_L.
6. The ratio N_I/N_L may be a measure of the film's effectiveness in inhibiting bacteria.

Declarations

Acknowledgments

The author would like to thank the Damascus University and the Syrian Atomic Energy Commission for providing the facility to carry out this research. He would also like to thank Dr. A. Alkhawwam for the assistance during working on the Microwave SAIREM GMP 20 KEDS system.

Funding

Not applicable

Competing Interests

Not applicable

Availability of data and materials

Not applicable

Code availability

Not applicable

Ethical Approval

This is an observational study. No ethical approval is required.

Consent to Participate

Not applicable

Consent to Publish

Not applicable

References

1. Zhou Jian-HongQPeng, Gao X-Y, Yu J-N, Wang S-Y, Li J, Zheng Y-X, Yang Y-M (2005) Qing-Hai Song and Liang-Yao, Chen_Ellipsometric Study of the Optical Properties of Silver Oxide Prepared by Reactive Magnetron Sputtering. Journal of the Korean Physical Society 46:269_S275
2. Wei N, Cui H, Song Q, Zhang L, Song X, Wang K, Li YZhang,Jian, Wen J, Tian J (2016) Ag_2O nanoparticle/TiO_2 nanobelt hetero structures with remarkable pphoto-response and photocatalytic properties under UV, visible and near-infrared irradiation. Appl Catal B 198:83–90
3. Zheng J, Dickson RM (2002) Individual Water-Soluble Dendrimer-Encapsulated Silver Nanodot Fluorescence. J Am Chem Soc 124:13982
4. Chunhua Liu X, Yang H, Yuan Z, Zhou (2007) Dan Xiao, Preparation of Silver Nanoparticle and Its Application to the Determination of *ct*-DNA. Sensors 7:708–718
5. Maalia A, Cardinal T, Treguer-Delapierre M (2003) Intrinsic putrescence from individual silver nanoparticles. Physica E 17:559–560
6. Lakowicz J (2013) Principles Of Fluorescence Spectroscopy, 3rd edn. Springer, New York, p 954
7. Wu K, Bera A, Ma C, Du Y, Yang Y, Li L et al, Temperature-dependent excitonic photoluminescence of hybrid organ metal halide perovskite films, Phys. Chem. Chem. Phys. 16 (41) (2014) 22476_22481
8. deQuilettes DW, Koch S, Burke S, Paranji R, Shropshire AJ, Ziffer ME et al., Photoluminescence lifetimes exceeding 8 Ms and quantum yields exceeding 30% in hybrid perovskite thin films by ligand passivation, ACS Energy Lett. (2016) 1_7
9. Richter JM, Abdi-Jalebi M, Sadhanala A, Tabachnyk M, Rivett JPH, Pazos-Outo´ LM (2016) n, et al., Enhancing photoluminescence yields in lead halide perovskites by photon recycling and light out-coupling. Nat Commun 7:13941
10. Madhavi V, Kondaiah P, Mohan Rao G (2018) Influence of silver nanoparticles on titanium oxide and nitrogen doped titanium oxide thin films for sun light photocatalysis. Appl Surf Sci 436:708–719
11. Kamal Kumar Paul1, Ghosh R, Giri PK, Mechanism of strong visible light photocatalysis by Ag_2O-nanoparticledecorated monoclinic TiO_2(B) porous. nanorodsNanotechnology 27 (2016) 315703 (15pp)
12. Samaila Buda S, Shafie SA, Rashid H, Jaafar NFM, Sharif (2017) Enhanced visible light absorption and reduced charge recombination in AgNP plasmonic photo electrochemical cell. Results in Physics 7:2311–2316
13. Zhang A, Zhang J, Fang Y (2008) Photoluminescence from colloidal silver nanoparticles. J Lumin 128:1635–1640

14. Kayed K. The Optical Properties of Individual Silver Nanoparticles in Ag/Ag_2O Composites Synthesized by Oxygen Plasma Treatment of Silver Thin Films. *Plasmonics* (2020) https://doi.org/10.1007/s11468-020-01169-9
15. Born M, Wolf E, Principles of Optics, 6th edition, Cambridge University Press (2005)
16. Perkins JD, Teplin CW, van Hest MFAM, Alleman JL, Li X, Dabney MS, Keyes BM, Gedvilas LM, Ginley DS, Lin Y, Lu Y (2004) Optical analysis of thin film combinatorial libraries. Appl Surf Sci 223:124–132
17. Kayed K (2018) Effect of nitrogen plasma afterglow on the surface charge effect resulted during XPS surface analysis of amorphous carbon nitride thin films. Spectrochim Acta Part A Mol Biomol Spectrosc 199:242–247
18. Kayed K (2018) Effect of nitrogen plasma afterglow on the (1000–1800) cm^{-1} band in FTIR spectra of amorphous carbon nitride thin films. Spectrochim Acta A Mol Biomol Spectrosc 190:253–258
19. Kayed K (2021) The luminescence properties of individual silver nanoparticles in Ag/Ag_2O composites synthesized by oxygen plasma treatment of silver thin films. J Lumin 237:118163
20. Kayed K The Mirror Image Symmetry in the Optical Absorption/Luminescence Spectra of Silver Nanoparticles in Ag/Ag_2O Composites Synthesized by Oxygen Plasma Treatment of Silver Thin Films. Plasmonics (2021) https://doi.org/10.1007/s11468-021-01489-4
21. Kayed K, Alberni L (2020) The Effect of Annealing Temperature on the Plasma Edge in Reflectance Spectra of Al/Al_2O_3 Composites Synthesized by Thermal Oxidation of Aluminum Thin Films. Plasmonics 15:1959–1966
22. Kayed K, Mansour L (2022) The Antimicrobial Activity of Silver Nanoparticles in Ag/Ag_2O Composites Synthesized by Oxygen Plasma Treatment of Silver Thin Films. Current Applied Science Technology 22:1–9

Figures

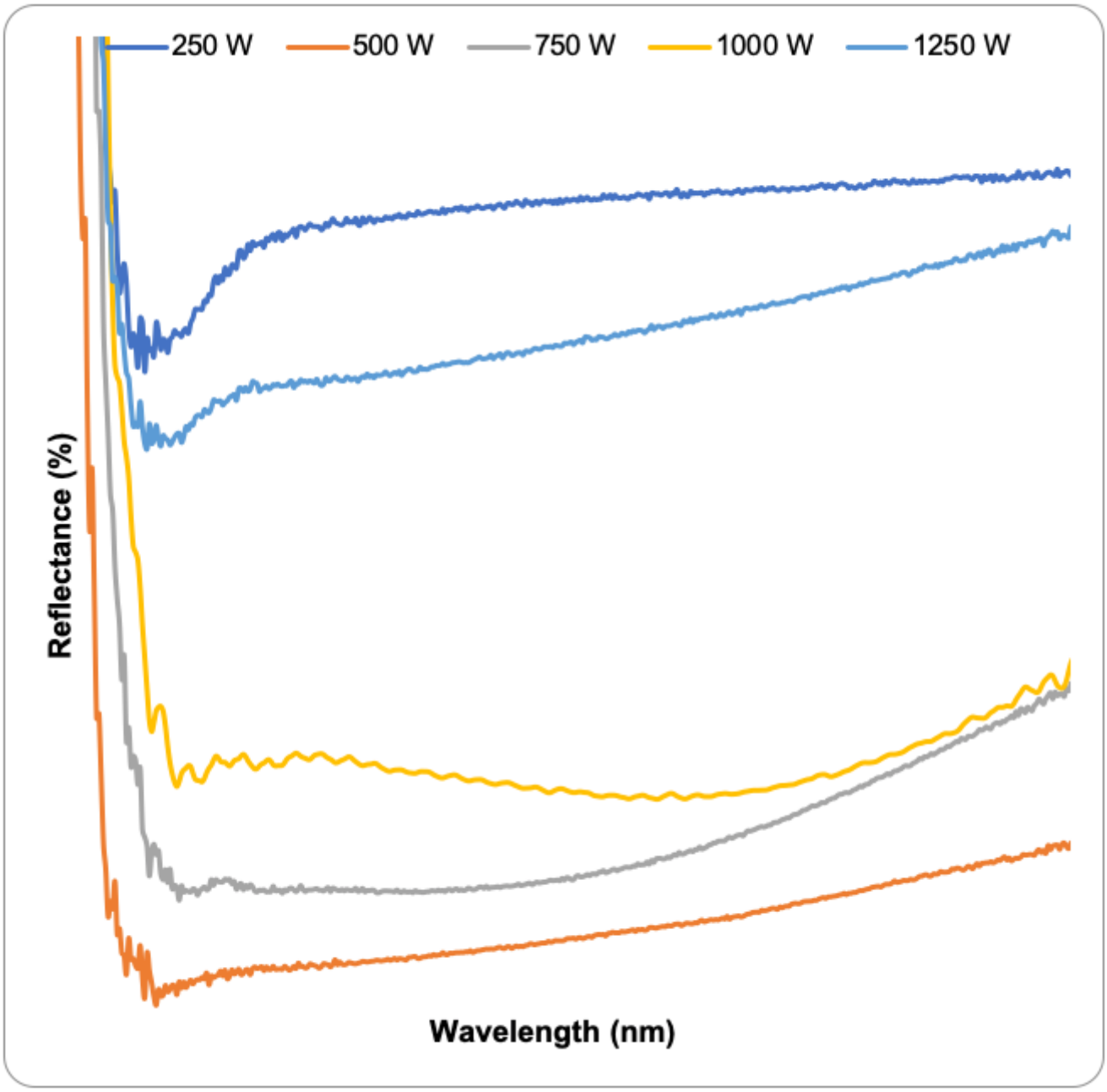

Figure 1

The reflectance spectra of the prepared Ag2O thin films.

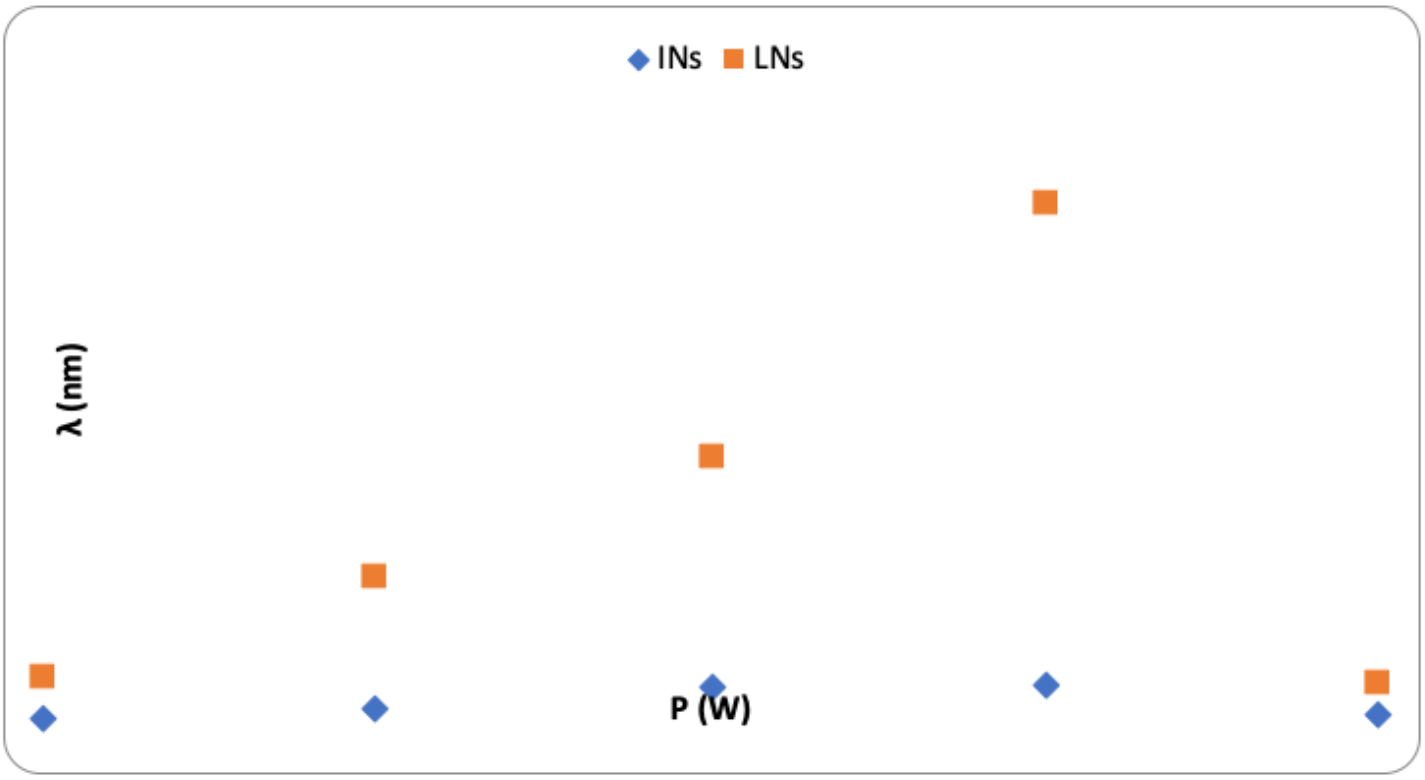

Figure 2

The two plasma edges as functions of plasma power.

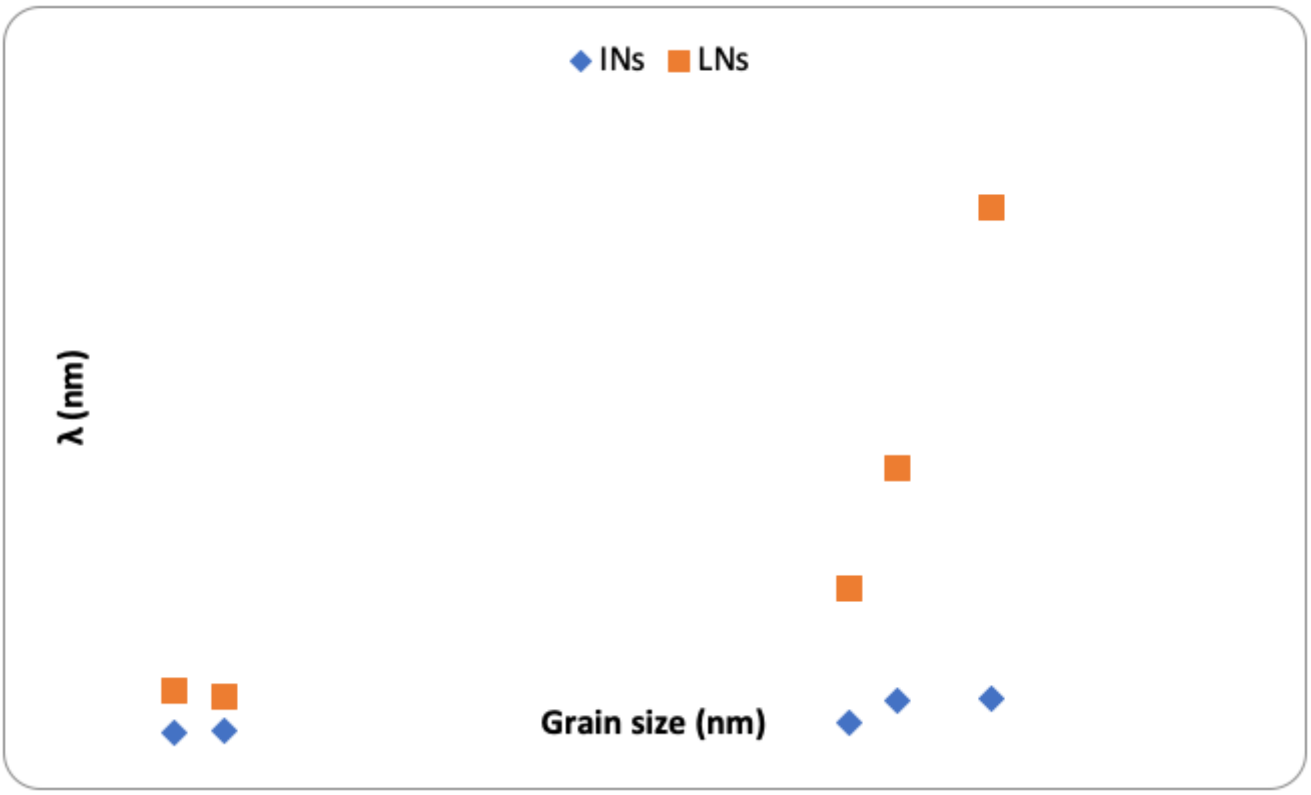

Figure 3

The two plasma edges as functions of grain size.

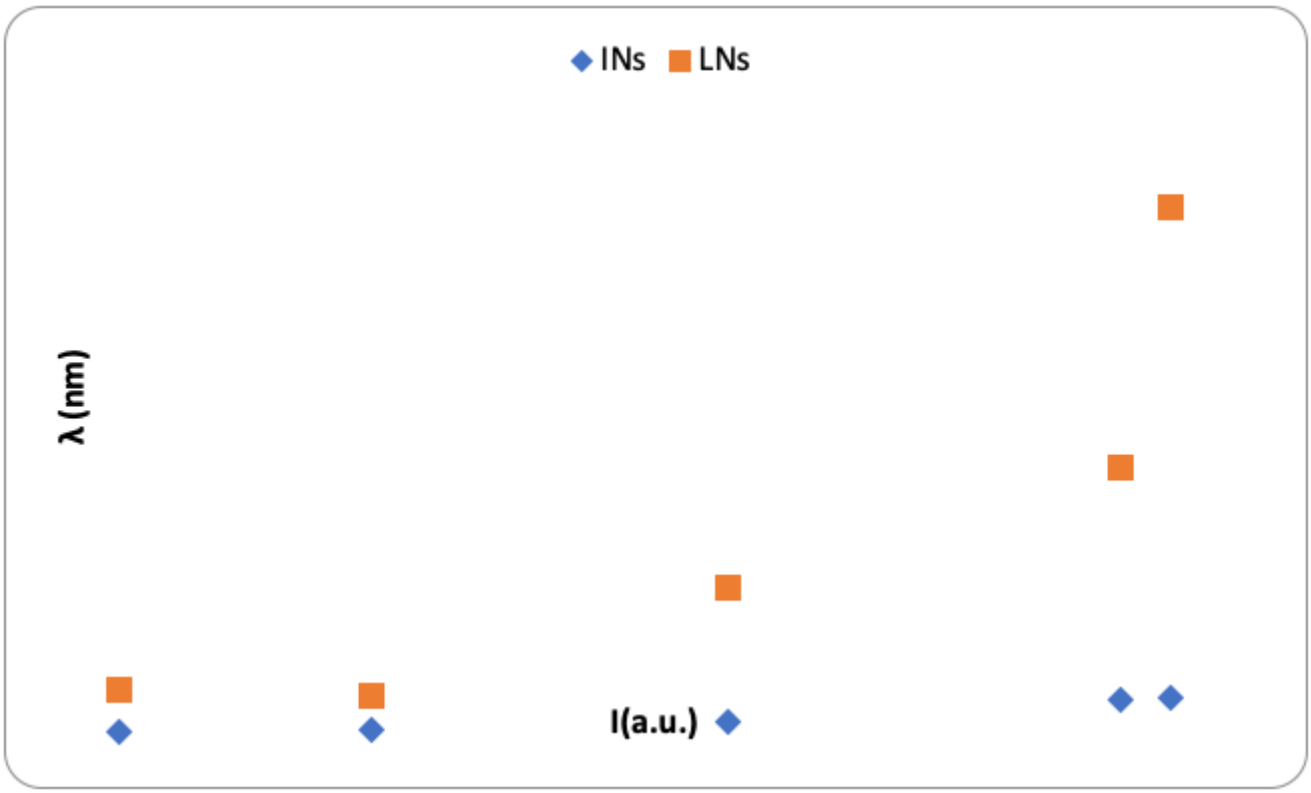

Figure 4

The two plasma edges as functions of silver oxide XRD peak intensity.

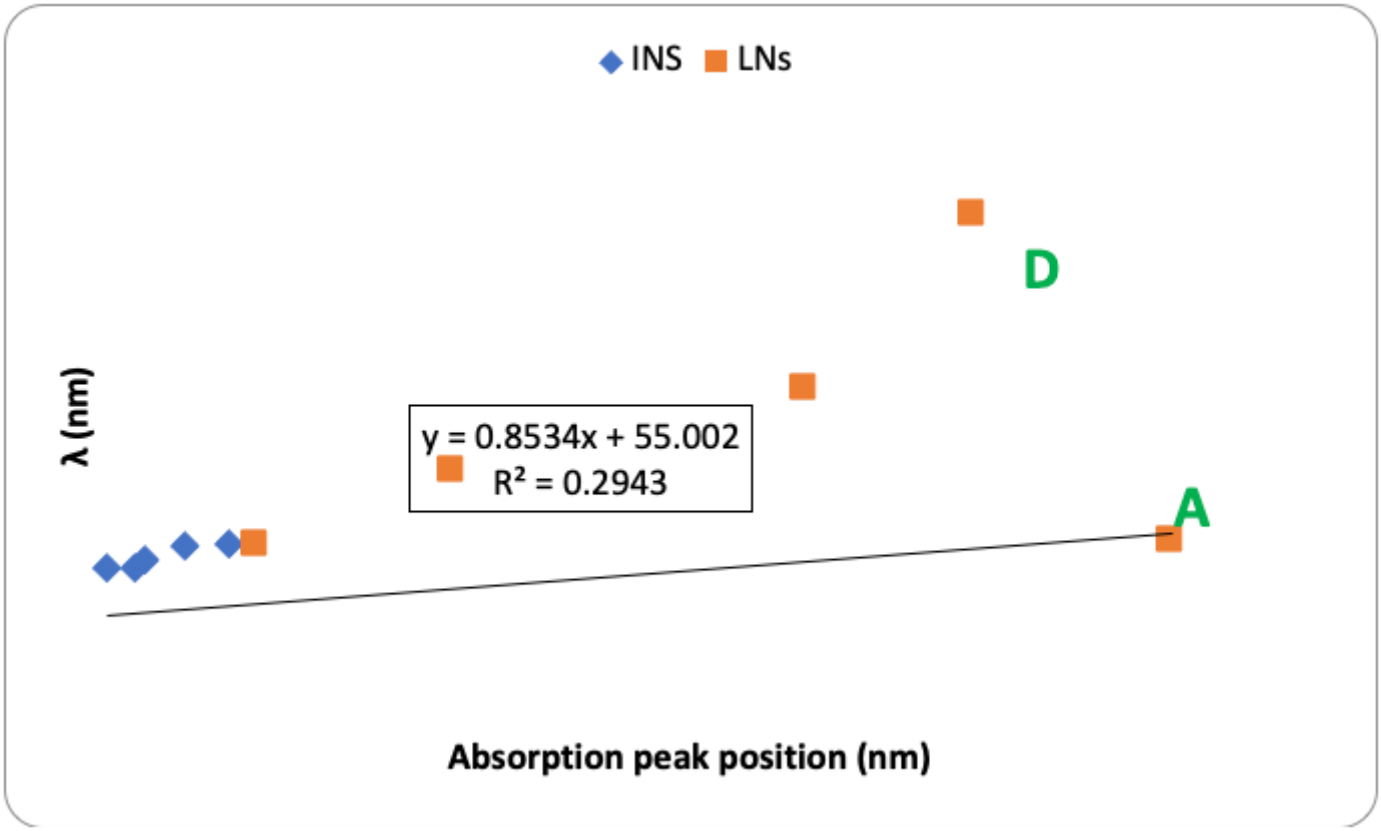

Figure 5

The plasma edge as functions of absorption peak position.

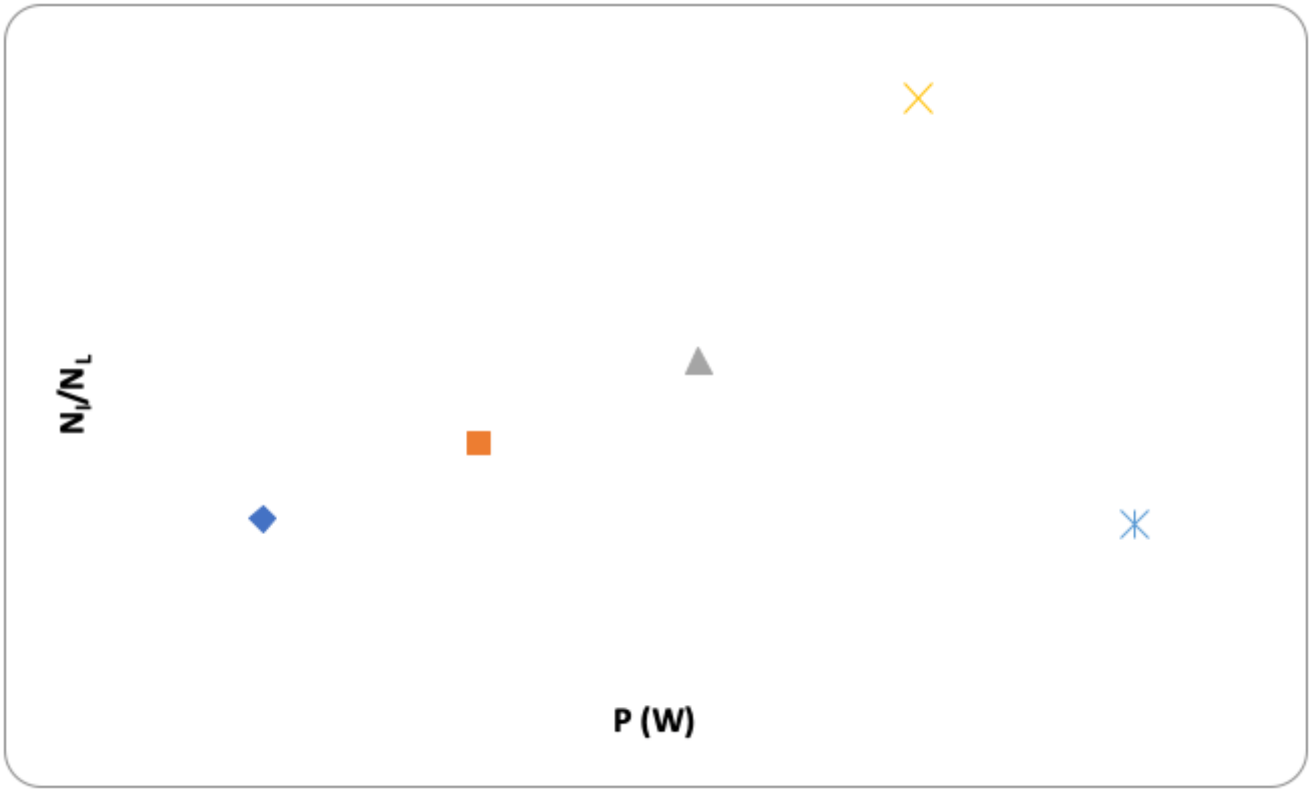

Figure 6

The ratio NI/NL as functions of plasma power.

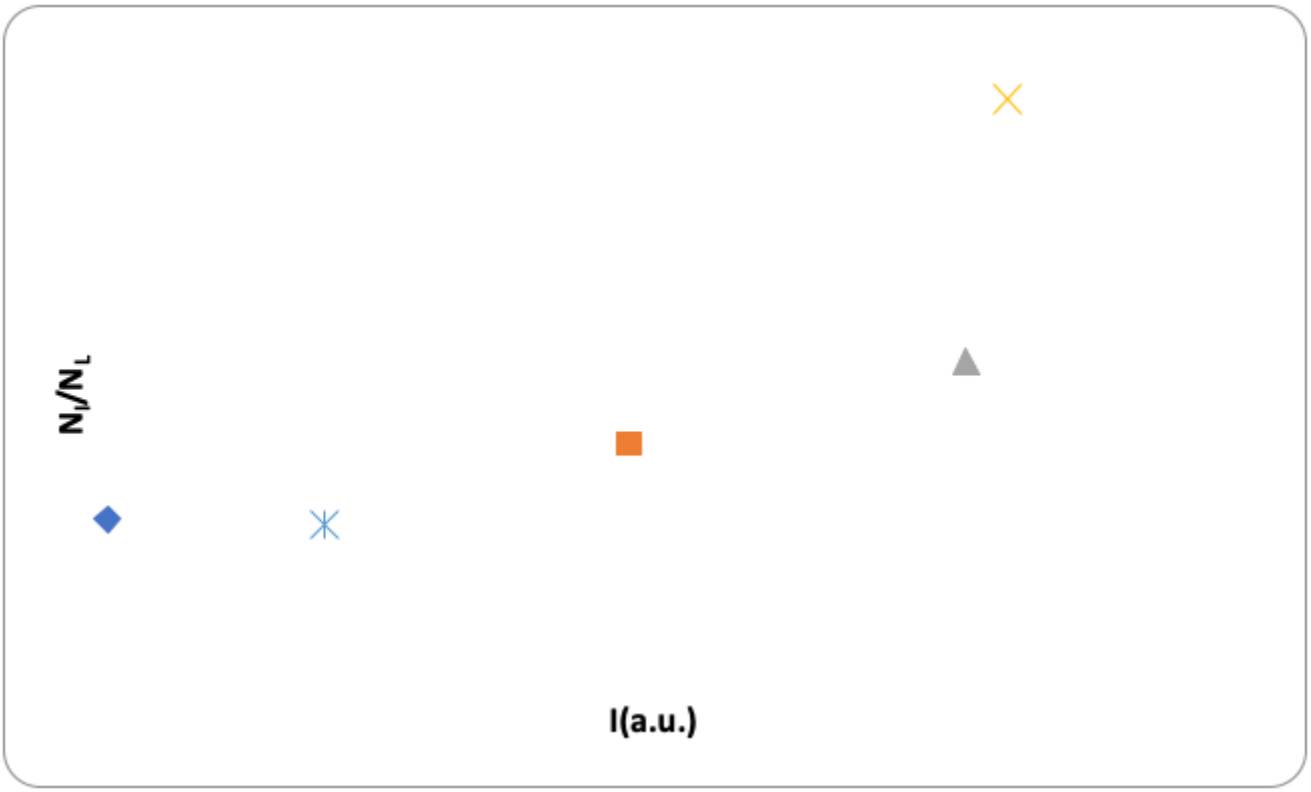

Figure 7

The ratio NI/NL as functions of silver oxide XRD peak intensity.

Figure 8

The ratio NI/NL as functions of grain size.